


Magnon-Phonon-Interaction-Induced Electromagnetic Wave Radiation in the Strong-Coupling Region

Yahui Ji, Chenye Zhang, and Tianxiang Nan^{✉*}

School of Integrated Circuits and Beijing National Research Center for Information Science and Technology (BNRist), Tsinghua University, Beijing 100084, China

 (Received 29 April 2022; revised 15 October 2022; accepted 17 November 2022; published 16 December 2022)

We theoretically study the electromagnetic wave radiation of magnons driven by acoustic phonons in systems with strong magnon-phonon interaction. We evaluate the field dependence of radiation intensity spectra that exhibits the avoided crossing, a characteristic of strongly coupled systems. At the crossover where the magnon and phonon eigenstates are hybridized, we demonstrate the existence of two resonant radiation frequencies with circular polarization and the enhancement of antenna radiation efficiency by over 100 times. We can also reconfigure the ellipticity of the antenna polarization by changing the applied out-of-plane magnetic field. Our results open up possibilities of developing ultracompact antennas by using the hybridized magnon-phonon mode.

DOI: [10.1103/PhysRevApplied.18.064050](https://doi.org/10.1103/PhysRevApplied.18.064050)

I. INTRODUCTION

Magnons are the quanta of spin waves, the collective excitation of magnetically ordered materials [1,2], which can be used for low-dissipation information processing and communications without moving charges [3–7]. Magnons can be excited by means of electrical currents or microwave pulses for the generation of electromagnetic (EM) waves [8–10]. The more efficient excitation of magnons can be realized in coupling with phonons, the quanta of lattice vibrations, which allows the hybridization of magnon and phonon modes in the strong-coupling region, referred to as a magnon-polaron [11–18]. Ferromagnetic magnons with their intrinsic magnetization dynamics in the GHz range can couple to mechanical vibrations at the same frequency generated from acoustic transducers, which has attracted growing attention in microwave devices [19–21]. However, the radiation of EM waves by utilizing magnon-phonon coupling has not been studied. Here we propose a magnon-polaron antenna that can radiate EM waves by magnetization precession driven by mechanical vibrations when magnetic and acoustic resonances are synchronized. Because such antennas are driven by acoustic resonances, their size is comparable to the acoustic wavelength and no longer limited by the EM wavelength, leading to a significant miniaturization of antennas.

This magnon-polaron antenna is in stark contrast to the recently demonstrated magnetoelectric (ME) antennas [22–26], since the EM radiation from ME antennas is far from the magnetic resonance condition, which is

evidenced by the insensitivity of radiation power to external magnetic fields [27,28]. In analytical models of ME antennas [29–31], although the Landau-Lifshitz-Gilbert (LLG) equation [32,33] that governs the micromagnetic dynamics has been considered [34–37], the theory of EM radiation induced by strong magnon-phonon coupling is elusive. It is expected that the hybridization of magnon and phonon modes can significantly boost the radiation power; however, the analytical model of EM wave radiation in the strong-coupling region has not been established.

Here, we theoretically investigate the EM wave radiation of magnetic resonances in a low-damping ferrimagnetic insulator driven by bulk acoustic waves (BAWs) using a one-dimensional multiscale finite-difference time-domain (FDTD) model. We show the frequency splitting of antenna radiation peaks resulting from magnon-phonon coupling when the magnetic resonance is brought into the acoustic resonance by tuning the external magnetic field. The field dependence of radiation intensity spectra exhibits the avoided crossing, which reveals the magnon and phonon dispersion relation at the crossover, a direct evidence of strongly coupled systems. At the magnon-polaron mode, the antenna radiation efficiency can be enhanced by over 100 times compared with that outside the strong-coupling region. In addition, we demonstrate that the antenna polarization mode can be reconfigured from circular to elliptical polarization depending on the strength of applied out-of-plane magnetic fields.

II. NUMERICAL METHODS

The magnon-polaron antenna structure and the EM wave radiation mechanism are illustrated in Fig. 1(a). The

*nantianxiang@mail.tsinghua.edu.cn

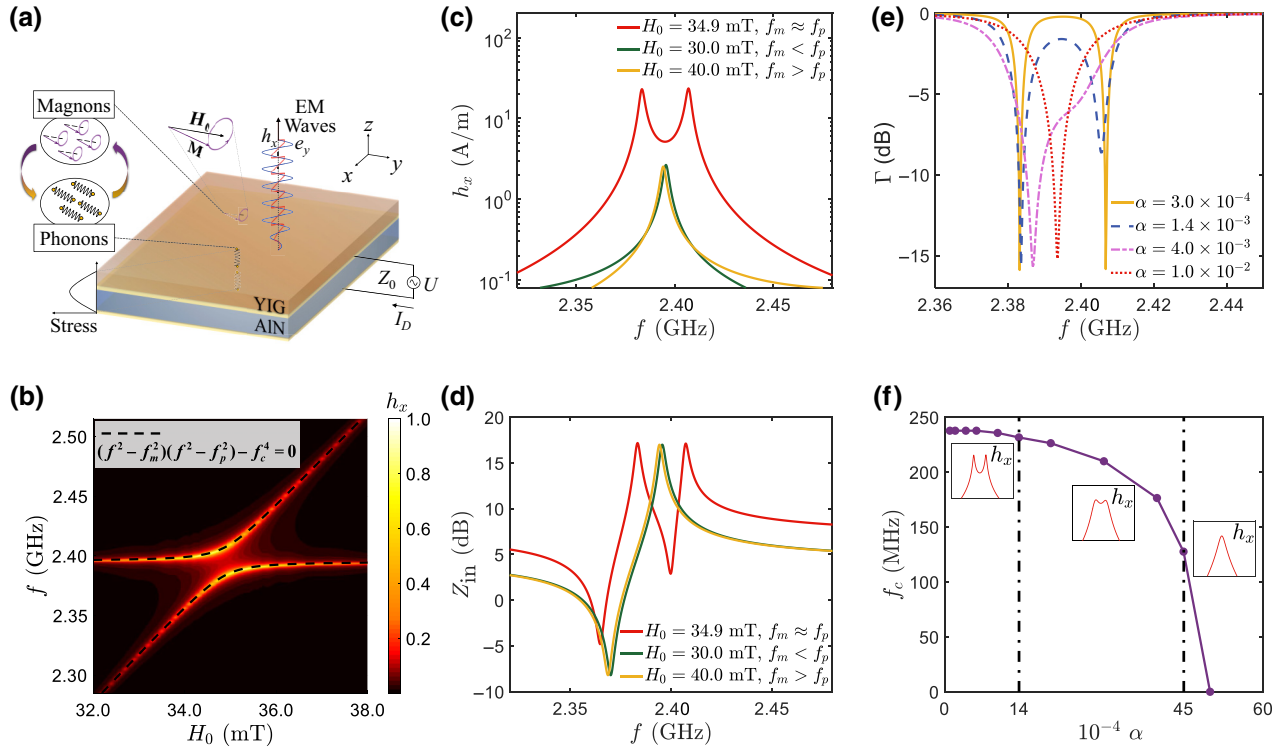


FIG. 1. (a) Schematic of the proposed magnon-polaron antenna and the EM radiation mechanism. (b) Normalized Fourier amplitude spectra of radiation magnetic field (along the x axis) h_x as a function of the magnetic bias field H_0 . (c) Frequency spectra of h_x at different magnetic bias fields. (d) Frequency spectra of the input impedance $Z_{\text{in}} = U/I_D$ at different magnetic bias fields. (e) Frequency spectra of the reflection coefficient $\Gamma = (Z_{\text{in}} - Z_0) / (Z_{\text{in}} + Z_0)$ for various Gilbert damping constants α of YIG. (f) Magnon-phonon coupling factor f_c as a function of α . The insets are the representative radiation field spectra with different α .

antenna is composed of a ferrimagnetic/piezoelectric heterostructure, in which a voltage excitation U is applied on the piezoelectric layer to stimulate a mechanical vibration that can be immediately transferred to the upper ferrimagnetic layer. This consequently produces a bulk acoustic wave along the z direction of the heterostructure. An in-plane magnetic bias field H_0 is applied in the y direction to saturate the magnetization and modify the ferromagnetic resonance (FMR) frequency. Due to the strain-mediated ME coupling, the piezoelectric driven oscillating strain induces magnetization dynamics \mathbf{M} in the magnetostrictive layer whose precession is governed by the LLG equation as

$$\frac{\partial \mathbf{M}}{\partial t} = \mu_0 \gamma (\mathbf{M} \times \mathbf{H}_{\text{eff}}) - \frac{\alpha}{|\mathbf{M}|} \mathbf{M} \times \frac{\partial \mathbf{M}}{\partial t}, \quad (1)$$

where μ_0 , γ , and α are the permeability of vacuum, the gyromagnetic ratio constant, and the Gilbert damping constant, respectively. \mathbf{H}_{eff} is the effective magnetic field, which includes the magnetic bias field H_0 , the radiation magnetic field \mathbf{H} , and the piezomagnetic induced field H_m . When the magnon and phonon modes are hybridized, the magnon-polarons efficiently radiate EM fields \mathbf{E} and \mathbf{H} with dynamic components e_y and h_x propagating into free

space, which is described by Maxwell's equations as

$$\nabla \times \mathbf{H} = \varepsilon_r \varepsilon_0 \frac{\partial \mathbf{E}}{\partial t}, \quad (2)$$

$$\nabla \times \mathbf{E} = -\mu_0 \frac{\partial (\mathbf{H} + \mathbf{M})}{\partial t}, \quad (3)$$

where ε_0 and ε_r are the permittivity of vacuum and the relative dielectric constant, respectively. In our FDTD model, the LLG equation and Maxwell's equations are interactively coupled with Newton's equations that govern the dynamics of acoustic waves (see Supplemental Material [38] for a detailed description of the FDTD model).

III. RESULTS

A. Strong magnon-phonon coupling

We choose a model system of aluminum nitride (AlN)/yttrium iron garnet (YIG) heterostructure, because AlN thin film is a widely used piezoelectric material for BAW resonators [39] and YIG is the benchmark ferromagnetic insulator with ultralow damping [40–42]. In our 1- μm AlN/750-nm YIG heterostructure, the standing phonon mode or the mechanical resonance frequency f_p is governed by the thickness of AlN and the sound velocity

of YIG and AIN, which is simulated to be 2.39 GHz (see Supplemental Material [38] for the material parameters). The magnon mode or the FMR frequency f_m of YIG can be shifted by the in-plane magnetic bias H_0 following the Kittel equation $f_m = \mu_0\gamma/2\pi \sqrt{H_0(H_0 + M_s)}$, where M_s is the saturation magnetization. Figure 1(b) shows the calculated radiation field h_x as functions of magnetic bias field and frequency, which exhibits the avoided crossing, indicating the hybridization of magnon and phonon modes in the strong-coupling region and the formation of magnon-polarons. The numerically calculated field dependence of radiation spectra can be fitted to a characteristic equation for strongly coupled systems: $(f^2 - f_m^2)(f^2 - f_p^2) - f_c^4 = 0$, where f_c is the coupling factor [43,44]. The coupling factor that determines the strength of the magnon-phonon coupling is directly associated with the magnetostriction coefficient, the magnetic moment, and wave vectors of magnons and phonons [45].

To evaluate the radiation properties of the magnon-polaron antenna, we compare the frequency spectra of the radiation field [Fig. 1(c)] and the input impedance $Z_{in} = U/I_D$ [Fig. 1(d)] at different magnetic bias fields. When f_m is away from f_p ($f_m < f_p$ or $f_m > f_p$), one radiation peak is presented in Fig. 1(c), which corresponds to the mechanical resonance in Fig. 1(d) at the same frequency. This is consistent with what has been observed in ME antennas [27,28]. As the magnon resonance is brought closer to the phonon resonance ($f_m \approx f_p$), the radiation peak is split into two peaks [Fig. 1(c)] with their intensities enhanced by over 10 dB, which leads to possible applications of magnon-polaron antennas with radiation field much higher than that of ME antennas. Interestingly, in the hybridized mode, the impedance spectra also show two mechanical resonances [Fig. 1(d)], because the hybridized mode does not exist in a specific eigenstate, but rather has both magnonic and phononic characters. The impedance measurement of magnon-phonon systems might therefore serve as a sensitive probe for the observation of magnon-phonon dynamics.

The antenna resonance of the hybridized mode is sensitive to the Gilbert damping constant, since the magnon-phonon coupling strongly depends on the loss rate of the system. To better illustrate the evolution of antenna resonance characteristics, we show the spectra of the reflection coefficient defined as $\Gamma = (Z_{in} - Z_0) / (Z_{in} + Z_0)$ for various Gilbert damping constants α in Fig. 1(e), where Z_0 is the characteristic impedance of 50 Ω . As the Gilbert damping constant increases from 3.0×10^{-4} (typical damping constant of YIG) to 1.0×10^{-2} (typical damping constant of ferromagnetic metals), two symmetric resonances in Γ induced by the hybridized mode are gradually merged into one resonance solely induced by the phonon mode. Figure 1(f) summarizes the magnon-phonon coupling factor f_c and the corresponding representative profiles of radiation field spectra as a function of Gilbert damping

constants α . We find that the magnon-phonon coupling factor f_c drastically decreases when α exceeds 1.4×10^{-3} , which implies a thresholdlike behavior.

B. Enhanced radiation efficiency

We calculate the antenna radiation efficiency, which is defined by the ratio of the radiated power per unit area to the input power per unit area, as

$$\eta_{\text{rad}} = \frac{P_{\text{rad}}}{P_{\text{in}}} = \frac{\frac{1}{2}\eta_0 |h_x| \times |h_x|}{\frac{1}{2}\text{Re}[U \times J_D^*]}, \quad (4)$$

where η_0 is the intrinsic impedance of free space and J_D is the displacement current density. It should be noted that the radiation efficiency here is independent of the shape and size of antennas, because our model is in one dimension. We evaluate the radiation efficiency of the magnon-polaron antenna with and without the hybridization mode by taking proper loss mechanisms into account. For conventional antennas, the radiation efficiency is determined by the Ohmic loss, while for the magnon-polaron antenna, the radiation efficiency is dominated by the mechanical viscosity and the magnetic damping. We consider a reasonable mechanical quality factor of the acoustic structure to be around 500 and the Gilbert damping constant of YIG to be 3.0×10^{-4} in numerical simulation. Figure 2 shows the antenna radiation efficiency as a function of magnetic bias field H_0 . Beyond the strong-coupling region, the radiation efficiency is of the order of 0.04%. While in the strong-coupling region, the radiation efficiency can be enhanced by over 2 orders of magnitude with a maximum value of around 7.0%. When $f_m \approx f_p$ at $H_0 = 34.9$ mT, the new eigenfrequencies are $f_p \pm g$, where the frequency splitting g is related to f_c as $g = f_c^2/2f_p$. The strong magnon-phonon coupling starts at $H_0 = 34.5$ mT ($f_m = f_p - g$) and ends at $H_0 = 35.3$ mT ($f_m = f_p + g$), spanning across a field range of 0.8 mT. We note that the antenna radiation efficiency is mainly affected by magnetostriction and phonon damping in the noncoupling region, while being mainly affected by phonon damping and magnon damping in the strong-coupling region (see Supplemental Material [38] for the analytical radiation efficiencies versus the magnetostriction constant, the mechanical viscosity constant, and the Gilbert damping constant).

C. Circularly polarized radiation

To study the polarization modes of antennas, the x and y components of the radiation field need to be simultaneously analyzed. We construct an out-of-plane magnetic bias field model, which allows us to calculate the radiation magnetic field h_x and h_y (see Supplemental Material [38]). Under the out-of-plane magnetic field bias as shown in Fig. 3(a), the hybridization of magnon and phonon modes

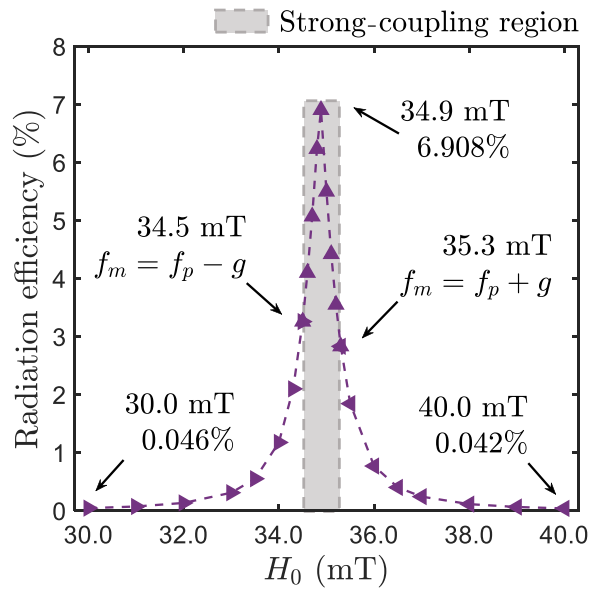


FIG. 2. Antenna radiation efficiency as a function of magnetic bias field H_0 . Beyond the strong-coupling region, we drive at the mechanical resonance frequency corresponding to each H_0 , which is very near the intrinsic phonon frequency f_p . In the strong-coupling region with two obvious radiation peaks, we drive the radiation peak of strong mechanical resonance whose frequency is much closer to f_p . When $f_m \approx f_p$ at $H_0 = 34.9$ mT, we drive at $f_p \pm g$, and their radiation efficiencies are 7.309% and 6.908%, respectively. We illustrate the efficiency of 6.908% at $H_0 = 34.9$ mT.

takes place in a different field region since the FMR condition is different with the in-plane scenario. We find that the polarization modes are strongly dependent on the magnetic bias field, where Figs. 3(b)–3(d) show the evolution of the antenna polarization mode with increasing magnetic field across the strong-coupling region. In the strong-coupling region ($f_m \approx f_p$), right-hand circular polarization is observed. Such polarization mode induced by magnon-phonon coupling is in sharp contrast to ME antennas, which have been demonstrated to have linear polarization [27]. From the antenna application point of view, circularly polarized antennas are of special interest as EM transmitting and receiving are locally omnidirectional, which can combat signal fading from a pair of misaligned linearly polarized antennas [46]. Outside the strong-coupling region ($f_m \neq f_p$), the magnon-polaron antenna shows right-hand elliptical polarization, in which the axial ratio (AR) of elliptical polarization (the ratio between radiation field amplitude of long axis and short axis) strongly depends on the out-of-plane magnetic bias field. These behaviors can be attributed to the circular or elliptical magnetization precession under different magnetic bias fields. The numerical results of the polarization mode with both isotropic and anisotropic magnetostriction constant are in a good

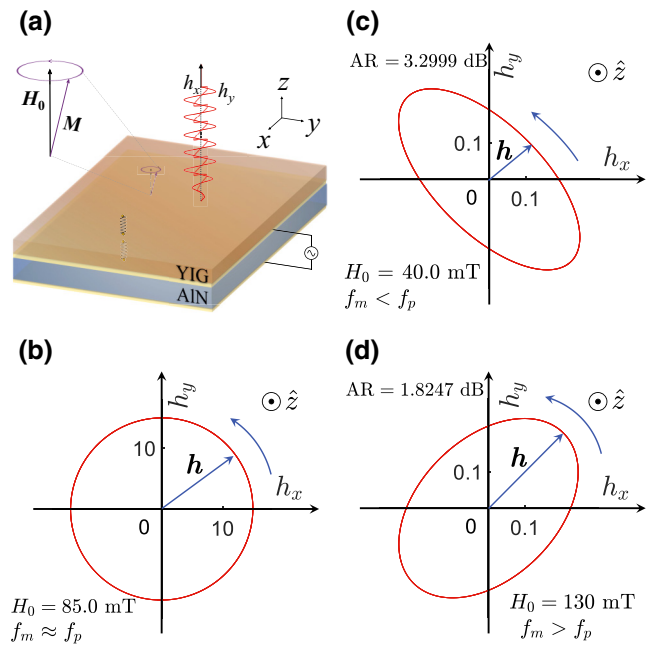


FIG. 3. (a) Schematic of magnon-polaron antenna under out-of-plane magnetic bias field. Polarization modes of the antenna under different out-of-plane magnetic bias fields of (b) 85.0 mT with $f_m \approx f_p$, (c) 40.0 mT with $f_m < f_p$, and (d) 130 mT with $f_m > f_p$. The unit of h_x and h_y is A/m. Note that the radiation field strength in (b) is about 100 times larger than that in (c) and (d).

agreement with our analytical calculations (see Supplemental Material [38]). The magnetic-field-tunable polarization mode in the magnon-polaron antenna suggests applications in reconfigurable antennas [47,48].

IV. CONCLUSION AND DISCUSSION

We theoretically demonstrate that hybridized magnon-phonon dynamics can lead to efficient EM wave radiation in a ferrimagnetic/piezoelectric heterostructure. In the strong magnon-phonon coupling region, we show that the antenna radiation efficiency can be enhanced by 2 orders of magnitude. The formation of magnon-polarons leads to the frequency splitting of antenna radiation peaks, which can be tuned by engineering the magnetostriction coefficient or the Gilbert damping constant of the magnets. Such dual splitting resonances can be used to transmit binary information with frequency shift keying modulation [49], which effectively broadens the bandwidth of the antenna. Our results are in sharp contrast to those for ME antennas in which the magnetic and acoustic resonances are significantly mismatched. The magnon-polaron-induced EM radiation opens up intriguing perspectives for developing highly efficient electrically small antennas that have a size comparable to the acoustic wavelength, and sheds light on magnonic devices for information communications.

We briefly discuss the experimental realization of a magnon-polaron antenna with hybridized modes. It is challenging to achieve high-quality epitaxial AlN/YIG heterostructures because of large lattice mismatch [50]. Free-standing single-crystalline YIG membranes with ultralow damping can be used to construct AlN/YIG heterostructures [51,52]. On the other hand, metallic ferromagnetic thin-film materials with generally large magnetostriction constant and low damping constant comparable to those of YIG such as Co-Fe alloys are alternatives [53], which can be directly sputtered on the AlN layer.

ACKNOWLEDGMENTS

We thank Jiamian Hu and Shihao Zhuang at the University of Wisconsin, Madison for a critique of the initial draft of this paper and their helpful suggestions. We acknowledge Zhi Yao at the University of California, Los Angeles (UCLA) for her groundbreaking contributions to numerical models of BAW antennas. This work is supported by the National Key R&D Program of China (Grant No. 2021YFA0716500), the National Natural Science Foundation (Grants No. 52073158, No. 52161135103, and No. 62131017), and the Beijing Advanced Innovation Center for Future Chip (ICFC).

-
- [1] V. V. Kruglyak, S. O. Demokritov, and D. Grundler, Magnonics, *J. Phys. D Appl. Phys.* **43**, 264001 (2010).
- [2] A. A. Serga, A. V. Chumak, and B. Hillebrands, YIG magnonics, *J. Phys. D Appl. Phys.* **43**, 264002 (2010).
- [3] A. V. Chumak, A. A. Serga, and B. Hillebrands, Magnon transistor for all-magnon data processing, *Nat. Commun.* **5**, 4700 (2014).
- [4] A. V. Chumak, V. I. Vasyuchka, A. A. Serga, and B. Hillebrands, Magnon spintronics, *Nat. Phys.* **11**, 453 (2015).
- [5] G. Csaba, A. Papp, and W. Porod, Perspectives of using spin waves for computing and signal processing, *Phys. Lett. A* **381**, 1471 (2017).
- [6] A. Mahmoud, F. Ciubotaru, F. Vanderveken, A. V. Chumak, S. Hamdioui, C. Adelman, and S. Cotozana, Introduction to spin wave computing, *J. Appl. Phys.* **128**, 161101 (2020).
- [7] P. Pirro, V. I. Vasyuchka, A. A. Serga, and B. Hillebrands, Advances in coherent magnonics, *Nat. Rev. Mater.* **6**, 1114 (2021).
- [8] M. Tsoi, Electromagnetic wave radiation by current-driven magnons in magnetic multilayers (invited), *J. Appl. Phys.* **91**, 6801 (2002).
- [9] O. Dzyapko, V. E. Demidov, S. O. Demokritov, G. A. Melkov, and V. L. Safonov, Monochromatic microwave radiation from the system of strongly excited magnons, *Appl. Phys. Lett.* **92**, 162510 (2008).
- [10] V. I. Vasyuchka, A. A. Serga, C. W. Sandweg, D. V. Slobodianiuk, G. A. Melkov, and B. Hillebrands, Explosive Electromagnetic Radiation by the Relaxation of a Multimode Magnon System, *Phys. Rev. Lett.* **111**, 187206 (2013).
- [11] E. G. Spencer and R. C. LeCraw, Magnetoacoustic Resonance in Yttrium Iron Garnet, *Phys. Rev. Lett.* **1**, 241 (1958).
- [12] M. Pomerantz, Excitation of Spin-Wave Resonance by Microwave Phonons, *Phys. Rev. Lett.* **7**, 312 (1961).
- [13] T. Kobayashi, R. C. Barker, J. L. Bleustein, and A. Yelon, Ferromagnetoelastic resonance in thin films. I. Formal treatment, *Phys. Rev. B* **7**, 3273 (1973).
- [14] T. Kobayashi, R. C. Barker, and A. Yelon, Ferromagnetoelastic resonance in thin films. II. Application to nickel, *Phys. Rev. B* **7**, 3286 (1973).
- [15] O. Y. Belyaeva, S. N. Karpachev, and L. K. Zarembo, Magnetoacoustics of ferrites and magnetoacoustic resonance, *Sov. Phys. Usp.* **35**, 106 (1992).
- [16] S. Streib, N. Vidal-Silva, K. Shen, and G. E. W. Bauer, Magnon-phonon interactions in magnetic insulators, *Phys. Rev. B* **99**, 184442 (2019).
- [17] Y. Li, W. Zhang, V. Tyberkevych, W.-K. Kwok, A. Hoffmann, and V. Novosad, Hybrid magnonics: Physics, circuits, and applications for coherent information processing, *J. Appl. Phys.* **128**, 130902 (2020).
- [18] Y. Li, C. Zhao, W. Zhang, A. Hoffmann, and V. Novosad, Advances in coherent coupling between magnons and acoustic phonons, *APL Mater.* **9**, 060902 (2021).
- [19] M. Weiler, L. Dreher, C. Heeg, H. Huebl, R. Gross, M. S. Brandt, and S. T. B. Gönnenwein, Elastically Driven Ferromagnetic Resonance in Nickel Thin Films, *Phys. Rev. Lett.* **106**, 117601 (2011).
- [20] O. Kovalenko, T. Pezeril, and V. V. Temnov, New Concept for Magnetization Switching by Ultrafast Acoustic Pulses, *Phys. Rev. Lett.* **110**, 266602 (2013).
- [21] X. Zhang, G. E. W. Bauer, and T. Yu, Unidirectional Pumping of Phonons by Magnetization Dynamics, *Phys. Rev. Lett.* **125**, 077203 (2020).
- [22] J. P. Domann and G. P. Carman, Strain powered antennas, *J. Appl. Phys.* **121**, 044905 (2017).
- [23] M. Zaeimbashi, H. Lin, C. Dong, X. Liang, M. Nasrollahpour, H. Chen, N. Sun, A. Matyushov, Y. He, X. Wang, C. Tu, Y. Wei, Y. Zhang, S. S. Cash, M. Onabajo, A. Shrivastava, and N. Sun, NanoNeuroRFID: A wireless implantable device based on magnetoelectric antennas, *IEEE J. Electromagn. RF Microwaves Med. Biol.* **3**, 206 (2019).
- [24] A. E. Hassanien, M. Breen, M.-H. Li, and S. Gong, A theoretical study of acoustically driven antennas, *J. Appl. Phys.* **127**, 014903 (2020).
- [25] H. Chen, X. Liang, C. Dong, Y. He, N. Sun, M. Zaeimbashi, Y. He, Y. Gao, P. V. Parimi, H. Lin, and N.-X. Sun, Ultra-compact mechanical antennas, *Appl. Phys. Lett.* **117**, 170501 (2020).
- [26] M. Nasrollahpour, A. Romano, N. Sun, M. Zaeimbashi, A. Matyushov, X. Liang, H. Chen, S. M. S. Abrishami, I. Martos-Repath, S. Emam, and N. X. Sun, Magneto-electric antenna for miniaturized acoustic noise dosimetry applications, *IEEE Sens. Lett.* **5**, 2500704 (2021).
- [27] T. Nan *et al.*, Acoustically actuated ultra-compact NEMS magneto-electric antennas, *Nat. Commun.* **8**, 296 (2017).
- [28] M. Zaeimbashi, M. Nasrollahpour, A. Khalifa, A. Romano, X. Liang, H. Chen, N. Sun, A. Matyushov, H. Lin, C. Dong, Z. Xu, A. Mittal, I. Martos-Repath, G. Jha, N. Mirchandani, D. Das, M. Onabajo, A. Shrivastava, S. Cash, and N. X. Sun, Ultra-compact dual-band smart NEMS

- magnetolectric antennas for simultaneous wireless energy harvesting and magnetic field sensing, *Nat. Commun.* **12**, 3141 (2021).
- [29] R. M. Bozorth and H. J. Williams, Effect of small stresses on magnetic properties, *Rev. Mod. Phys.* **17**, 72 (1945).
- [30] D. Davino, A. Giustiniani, and C. Visone, The piezomagnetic parameters of Terfenol-D: An experimental viewpoint, *Physica B* **407**, 1427 (2012).
- [31] S. W. Meeks and J. C. Hill, Piezomagnetic and elastic properties of metallic glass alloys $\text{Fe}_{67}\text{Co}_{18}\text{B}_{14}\text{Si}_1$ and $\text{Fe}_{81}\text{B}_{13.5}\text{Si}_{3.5}\text{C}_2$, *J. Appl. Phys.* **54**, 6584 (1983).
- [32] S. Zhuang, P. B. Meisenheimer, J. Heron, and J.-M. Hu, A narrowband spintronic terahertz emitter based on magnetoelastic heterostructures, *ACS Appl. Mater. Interfaces* **13**, 48997 (2021).
- [33] L. Bañas, Adaptive techniques for Landau–Lifshitz–Gilbert equation with magnetostriction, *J. Comput. Appl. Math.* **215**, 304 (2008).
- [34] Z. Yao, Master’s thesis, University of California, Los Angeles, 2014.
- [35] Z. Yao, Y. E. Wang, S. Keller, and G. P. Carman, Bulk acoustic wave-mediated multiferroic antennas: Architecture and performance bound, *IEEE Trans. Antennas Propag.* **63**, 3335 (2015).
- [36] Z. Yao, R. U. Tok, T. Itoh, and Y. E. Wang, A multiscale unconditionally stable time-domain (MUST) solver unifying electrodynamics and micromagnetics, *IEEE Trans. Microwave Theory Tech.* **66**, 2683 (2018).
- [37] Z. Yao, S. Tiwari, T. Lu, J. Rivera, K. Q. T. Luong, R. N. Candler, G. P. Carman, and Y. E. Wang, Modeling of multiple dynamics in the radiation of bulk acoustic wave antennas, *IEEE J. Multiscale Multiphys. Comput. Tech.* **5**, 5 (2019).
- [38] See Supplemental Material at <http://link.aps.org/supplemental/10.1103/PhysRevApplied.18.064050> for a detailed description of the FDTD model, the material parameters, the analytical radiation efficiencies, the out-of-plane magnetic bias field model, and the analytical calculations of polarization modes.
- [39] H. Bhugra and G. Piazza, *Piezoelectric MEMS Resonators* (Springer International Publishing, New York, 2017).
- [40] E. G. Spencer, R. C. LeCraw, and A. M. Clogston, Low-Temperature Line-Width Maximum in Yttrium Iron Garnet, *Phys. Rev. Lett.* **3**, 32 (1959).
- [41] V. Cherepanov, I. Kolokolov, and V. L’vov, The saga of YIG: Spectra, thermodynamics, interaction and relaxation of magnons in a complex magnet, *Phys. Rep.* **229**, 81 (1993).
- [42] H. Chang, P. Li, W. Zhang, T. Liu, A. Hoffmann, L. Deng, and M. Wu, Nanometer-thick yttrium iron garnet films with extremely low damping, *IEEE Magn. Lett.* **5**, 6700104 (2014).
- [43] L. Dreher, M. Weiler, M. Pernpeintner, H. Huebl, R. Gross, M. S. Brandt, and S. T. B. Gönnenwein, Surface acoustic wave driven ferromagnetic resonance in nickel thin films: Theory and experiment, *Phys. Rev. B* **86**, 134415 (2012).
- [44] C. Berk, M. Jaris, W. Yang, S. Dhuey, S. Cabrini, and H. Schmidt, Strongly coupled magnon-phonon dynamics in a single nanomagnet, *Nat. Commun.* **10**, 2652 (2019).
- [45] K. An, A. N. Litvinenko, R. Kohno, A. A. Fuad, V. V. Naleto, L. Vila, U. Ebels, G. de Loubens, H. Hurdequint, N. Beaulieu, J. Ben Youssef, N. Vukadinovic, G. E. W. Bauer, A. N. Slavin, V. S. Tiberkevich, and O. Klein, Coherent long-range transfer of angular momentum between magnon Kittel modes by phonons, *Phys. Rev. B* **101**, 060407(R) (2020).
- [46] F. Wu, J. Wang, Y. Zhang, W. Hong, and K.-M. Luk, A broadband circularly polarized reflectarray with magneto-electric dipole elements, *IEEE Trans. Antennas Propag.* **69**, 7005 (2021).
- [47] R. Simons, D. Chun, and L. Katehi, in *IEEE Antennas Propag. Soc. Int. Symp.* (IEEE, San Antonio, 2002), p. 6.
- [48] N. Ojaroudi Parchin, H. Jahanbakhsh Basherlou, Y. I. A. Al-Yasir, A. M. Abdulkhaleq, and R. A. Abd-Alhameed, Reconfigurable antennas: Switching techniques—A survey, *Electronics* **9**, 336 (2020).
- [49] M. A. Kemp, M. Franzi, A. Haase, E. Jongewaard, M. T. Whittaker, M. Kirkpatrick, and R. Sparr, A high Q piezoelectric resonator as a portable VLF transmitter, *Nat. Commun.* **10**, 1715 (2019).
- [50] J. Xu, C. Zhong, X. Zhou, X. Han, D. Jin, S. K. Gray, L. Jiang, and X. Zhang, Coherent Pulse Echo in Hybrid Magnonics with Multimode Phonons, *Phys. Rev. Appl.* **16**, 024009 (2021).
- [51] C. Mahender, T. P. Sumangala, R. Ade, A. Saranya, S. Prasad, and N. Venkataramani, Low-loss YIG thick films for microwave applications, *Ceram. Int.* **45**, 4316 (2019).
- [52] H. S. Kum *et al.*, Heterogeneous integration of single-crystalline complex-oxide membranes, *Nature* **578**, 75 (2020).
- [53] M. A. W. Schoen, D. Thonig, M. L. Schneider, T. J. Silva, H. T. Nembach, O. Eriksson, O. Karis, and J. M. Shaw, Ultra-low magnetic damping of a metallic ferromagnet, *Nat. Phys.* **12**, 839 (2016).